IEEE Access
Multidisciplinary | Rapid Review | Open Access Journal

Received 22 March 2023, accepted 2 April 2023, date of publication 10 April 2023, date of current version 13 April 2023.

Digital Object Identifier 10.1109/ACCESS.2023.3265958

RESEARCH ARTICLE

A Combined Method for Line Selection of Single Phase to Ground Fault in Compensated Distributions Based on Evidence Theory

JIE SUN[1], YAN WANG[1], YI SUN[1], FANGMING JIN[1], XINYU GAO[2], AND QINGQUAN JIA[2]

[1]Qiqihar Power Supply Branch, State Grid Heilongjiang Electric Power Company Ltd., Qiqihar 161005, China
[2]Key Laboratory of Power Electronics for Energy Conservation and Motor Drive of Hebei Province, Yanshan University, Qinhuangdao 066004, China

Corresponding author: Xinyu Gao (gaoxinyu258@126.com)

This work was supported in part by the Technology Project of State Grid Heilongjiang Electric Power Company Ltd., under Grant 522413220001.

ABSTRACT In order to improve reliability of distributions, the neutrals are usually insulated or compensated with Peterson coil. Thus, the currents of single-phase to ground fault are weak, leading to difficulty in fault line selection problem. This paper investigates an evidence theory based integrated fault line selection method which employs multiple fault components to improve the performances of selection for neutral compensated distributions. Aim of this method is through the fusion strategy of the multi-fold unreliable fault components to arrive at more reliable solution. Three kinds of fault components including the transient, the abrupt changing, and the damped DC are developed. Fault measures are introduced for each line to quantitatively describe the likelihood of the line being the fault line. The fault components are extracted by dual-tree complex wavelet and atom decomposition. And the algorithms of calculating fault measures for the three components are developed according to the principle of the fault. The basic probability assignment (BPA) functions of evidence theory are established with the cloud model algorithm of data driven. Examples validate that through fusion algorithm of the multifold fault components, the line selection is more robust and reliable to varied circumstance than utilizing individual component.

INDEX TERMS Fault line selection, evidence theory, dual-tree complex wavelet, atom decomposition, cloud model algorithm.

I. INTRODUCTION

The neutral points of power distributions are usually insulated or grounded with a Peterson coil to improve the reliability [1]. When single-phase to ground fault occurs, the fault current will flow through the stray capacitors of the phase to the ground. As the stray capacitors are small, the impedances of the fault path are high, thus the fault currents in such faults are small. We call such a fault as small current grounding fault (SCGF). Compared to short circuit faults, the SCGF is able to avoid the damage of large fault currents or the arcs to electrical apparatus and the systems. As the phase to ground faults are very frequently to be occurred in distributions. Therefore, neutral insulated or compensated are advantageous to improve the properties such as the reliability greatly [2]. Conventional over-current relaying is designed specifically for short circuits. However, a SCGF produce inadequate current to trigger conventional relaying system [3]. Although a SCGF is not necessary to be cleared immediately, but retaining in fault state for long time is dangerous to humans and equipment [2]. Therefore, it is necessary to clear the fault as soon as possible. As the fault characteristics of SCGF are weak, a specific technique should be developed for distinguishing and selecting the fault line from all the lines in the same bus, and give the guidance information to the personnel or trip the fault line directly.

The zero-sequence component (residual component) is the unique characteristics occurred in SCGF, and are usually used for the fault line selection [4]. The currents of SCGF are usually far smaller than the load currents, therefore, great errors

The associate editor coordinating the review of this manuscript and approving it for publication was Baoping Cai.

are inevitably brought for acquisition of those quantities. The variation of fault conditions, for example metallic fault, high impedance fault, arcing fault and unstable intermittent fault, and so on, will increase the difficulty of the problem further [5]. For compensated networks, the fundamental currents of residuals are no longer 90° leading to the voltages of residuals in the fault line, and thus are no longer useful for fault line selection [6]. Other components such as the direction of zero-sequences, and the transients were developed [6], [7]. But anyway, as the available components are small, problem of SCGF line selection need to be explored further.

Lots of works have been done to deal with the line selection problem. Roughly summarized, the present methods are mainly comprised of steady-state-based method, the transient-based methods, and the others. Literature [8] propose a selection method according to the trajectory of zero-sequence voltage to deal with the unbalanced parameters of three phases in the distributions. Literature [9] revealed that the phase angles between the voltage and the current of zero sequence in healthy lines are invariant while that in the fault line is variant as the fault resistor varies. Based on this phenomenon, a selection method was provided. Literature [10] employed the comparison of synchronized voltage and current for high impedance fault. Literature [11] used the fitted value of voltage and current sampling sequence to implement the fault line selection. This method was applicable for components either steady state or transient. Literature [12] considered the vague characteristics in distinguishing the fault line, and used fuzzy theory to establish fault line selection algorithm. Literature [12] proposed a selection method using signal injection to the distribution and monitoring the dynamic parameters of the injected frequency. Literature [13] mapped the fault dynamic signals to time-frequency diagram, and utilized GoogLeNet training network to improve the accuracy of selection. Literature [14] introduced the membership and the weight coefficient to form a combined criterion. Literature [15] used synchrophasor measurement technology for high-impedance fault identification. Literature [16] detected high impedance arc fault according to the randomness of both the harmonics and the waveform distortions. Literature [17] employed a real-time measurement of ground parameters. In the way of injecting a signal of certain frequency into the neutral point and extract the parameters to select the fault line. While [18] and [7] employed wavelet transform to deal with the transient signals and constructing intelligent system for line selection. A method of zero sequence current increment be purposed in [19], and find the fault line by searching the line which have the most ZSC variation. Due to the result of fault diagnosis could be difference at different times for the given identical fault symptoms. Literature [20] used a Dynamic Bayesian network to diagnose fault in modern industrial systems. Literature [21] purposed a sensor placement methodology based on discrete particle swarm algorithm to control the information redundancy in fault diagnosis. Literature [22] employed a fault diagnosis methodology based on method to solve the uncertainties in control systems. Literature [23] used D-S evidence theory to fuse three kind of fault information included: transient, abrupt ware and real power to diagnose the SCGF effectively. Literature [24] chose the Db6 wavelet to extract the transient signals, and taking advantage of multi criteria fusion to realize the fault line selection availably. Literature [25] introduced a method for high impedance fault based on the energy distribution of traveling wave full waveform and constructed a HIF criterion to detect the fault line. Aim at analyzing the transient model of non-solidly grounding fault. Literature [26] raised a method based on using ration and direction of phase transient current changes to detect the faulty section comprehensively. Literature [27] presented a fault line selection method based on signal injection, and employed all phase Fourier transform to improve the accuracy of line selection. Literature [28] purposed a method based on modified artificial bee colony optimization deep neural network to solve the problem of difficult to choose the fault line.

Although variety of methods had been presented in the literatures, the methods were established merely used one kind of components and thus were disadvantage to the adaptability to fault circumstances. Due to the fault components for SCGF are weak and the fault circumstances are uncertain, one component may be distinct in some cases, while they may be very weak in other cases. Therefore, establishing a method with a fix component is almost impossible to fit all SCGF circumstances. To improve the robustness of the SCGF selection, an integrated method has been proposed in this paper for compensated distributions employing evidence theory (ET) to combine the multiple fault components.

The contribution of this paper includes:

1. Proposed a fusion strategy to utilize multifold fault components for SCGF fault selection problem. Through the fusion effect of multifold fault components, the results concluded from the whole fault components are focused on the common supported solution, therefore the robustness to diverse fault circumstances was improved.

2. The ET-theory-based method was introduced to implement the fusion algorithm. The evidence pieces were derived from different fault components. Each line was assigned with a quantified fault evidence piece. With ET fusion, the final solution was created according to all the evidence pieces of each line, thus arrived at a more reliable solution.

3. The fault measures were introduced to quantitively describe the degree of each line seeming to be the fault line based on the fault characteristics. The fault measures were further converted to basic probability assignment (BPA) for fusion with ET. Quantitively calculation of fault measures instead of qualitatively decision was made, then the final result of selection was made by the fusion of ET.

4. The fault components are successfully extracted by the dual-tree complex wavelet and the atom decomposition algorithm. The BPA functions are constructed by cloud model

algorithm, which leads the BPAs originated from historical data instead of simply provided subjectively.

The rest of this paper is organized as follows. the equivalent circuit of the distribution for SCGF and the characteristics for SCGF are presented in Section II. The concept of fault measures is introduced and the algorithms of fault measures for extracting the transient components, abrupt changing component and damped DC component are established respectively in Section III. Section IV introduces the D-S evidence theory, and establishes the BPA function to combine the evidences. Section V presents simulation and real examples to validate the algorithm. Finally, main conclusions are drawn in Section VI.

II. CHARACTERISTICS OF SCGF IN COMPENSATED DISTRIBUTIONS

Generally, in case the grounding current is above 10 Ampere, the fault arc will be probably sustained. Therefore, in Chinese regulations, the limitation value is specified at 10 A. If the fault current is above 10A, a Peterson coil ought to be installed to compensate the fault current to avoid the reburning of the arc. The Peterson coil is usually in over-compensated of about 5%-10%.

A. EQUIVALENT CIRCUIT OF THE DISTRIBUTION FOR SCGF

When SCGF occurs in the compensated distribution, the zero-sequence fault loop will be established as shown in Fig. 1. As the zero-sequence impedances of all lines are capacitive, both the health lines and fault line behave capacitance model between the phase to ground. In Fig. 1, i_k is the zero-sequence currents (we call this currents as residual currents including in transient); d_k is the length of the health line k; d_f is the distance from fault site to the bus; r_0, l_0 and c_0 are the unit parameters of resistance, reactance and capacitance of the lines respectively. $R_f = r_0 \times d_f$, $L_f = l_0 \times d_f$, $C_f = c_0 \times d_f$ are the total resistance, reactance and capacitance of fault line from fault site to the bus, respectively; L_p is the reactance of Peterson coil; i_L is the compensating current of Peterson coil; u_{f0} is the residual voltage in fault site; i_{f0} is the fault current in the fault path; φ_m is the initial angle of the residual voltage.

The equivalent circuit in Fig. 1 can be diagramed as in Fig. 2. The steady state current is derived as

$$\begin{cases} I_{\mathrm{L}} = \sqrt{\dfrac{U_{\mathrm{m}}^2}{\omega^2\left(L_{\mathrm{p}} + \lambda L_f\right)^2 + (\lambda R)^2}} \approx \sqrt{\dfrac{U_{\mathrm{m}}^2}{\left(\omega L_{\mathrm{p}}\right)^2 + (\lambda R)^2}} \\ I_{\mathrm{C}} = C_f L_{\mathrm{p}} \omega^2 I_{\mathrm{L}} \end{cases} \tag{1}$$

In transient state, the differential equations are described as in Equ. (2).

$$\begin{cases} L = L_f + L_p \\ C_f L_p L_f \dfrac{d^3 i_L}{d^3 t} + (R_G + R_f) C_f L_p \dfrac{d^2 i_L}{d^2 t} + L \dfrac{d i_L}{dt} \\ \quad + (R_G + R_f) i_L = U_m \sin(\omega t + \varphi_m) \end{cases} \tag{2}$$

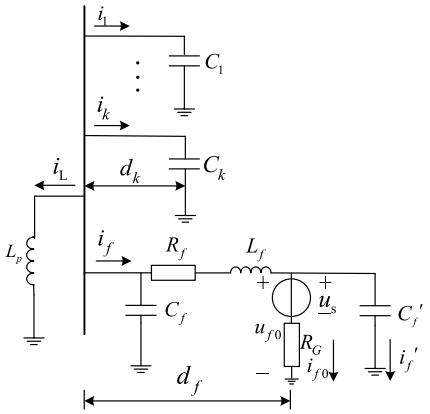

FIGURE 1. The zero-sequence circuit with SCGF.

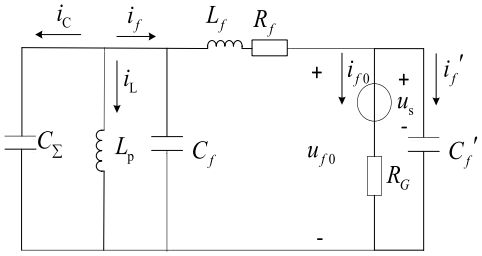

FIGURE 2. The SCGF equivalence of compensated distributions.

Solving the general solution of the differential equation, the transient characteristics are obtained.

B. CHARACTERISTICS ANALYSIS FOR SCGF

To solve differential equations in (2), if $R < \sqrt{R_1}$, the transient of residual currents of the health lines and the compensating current in Peterson coil are described in (3) and (4).

$$\begin{cases} i_{\mathrm{C}} = C_f L_{\mathrm{P}} I_{\mathrm{L}} \left(-\dfrac{r_1^2 r_2}{r_1 - r_2} \cos\varphi_{\mathrm{m}} \cdot e^{r_1 t} + k_1 e^{r_2 t} \right) \\ \quad + I_{\mathrm{C}} \cos(\omega t + \varphi_{\mathrm{m}}) \\ k_1 = \left[\dfrac{r_1}{r_1 - r_2} \left(r_2^2 - r_1^2 \right) \cos\varphi_{\mathrm{m}} - 2\omega r_2 \sin\varphi_{\mathrm{m}} \right] \cos\omega_2 t \\ \quad - \left[\dfrac{2 r_1 r_2 \omega}{r_1 - r_2} \cos\varphi_{\mathrm{m}} - \omega \dfrac{r_2^2 - \omega_2^2}{\omega_2} \sin\varphi_{\mathrm{m}} \right] \sin\omega_2 t \\ \quad - \dfrac{r_1^2 r_2 C_f L_{\mathrm{P}} I_{\mathrm{L}}}{r_1 - r_2} \cos\varphi_{\mathrm{m}} \cdot e^{r_1 t} \approx 0 \end{cases} \tag{3}$$

$$\begin{cases} i_{\mathrm{L}} = -\dfrac{r_2 I_{\mathrm{L}}}{r_1 - r_2} \cos\varphi_{\mathrm{m}} \cdot e^{r_1 t} + k_2 I_{\mathrm{L}} e^{r_2 t} - I_{\mathrm{L}} \cos(\omega t + \varphi_{\mathrm{m}}) \\ k_2 = \dfrac{r_1}{r_1 - r_2} \cos\varphi_{\mathrm{m}} \cos\omega_2 t - \dfrac{\omega}{\omega_1} \sin\varphi_{\mathrm{m}} \sin\omega_2 t \\ k_2 I_{\mathrm{L}} e^{r_2 t} \approx 0 \\ \dfrac{r_2}{r_1 - r_2} \approx -1 \end{cases} \tag{4}$$

where r_1 is the real eigen-root, and the r_2, ω_2 is the real part and the imaginary part of the imaginary eigen-root. According to the relationship of the quantities in the equivalent circuit, the current of fault line i_f is the negative sum of the currents in all health lines and in the coil, as described in (5)

$$i_f = -(i_C + i_L) \tag{5}$$

From (4) we know that the current in the coil is mainly composed of damped direct current (DC) component and the steady component; while the current in the health line is composed of the transient oscillating components and no DC component at all. Thus, the DC component will pass through the fault line. It equal to the DC component of the coil in magnitude and opposite in direction. The damped DC component is useful characteristic for line selection.

In case $\sqrt{R_1} < R < \sqrt{R_2}$ and $R > \sqrt{R_2}$, the damped oscillating components varied, but the DC component exists constantly. In addition, as the transient oscillating components exhibit high frequency, Peterson coil behaves high impedance and almost open for those components. Therefore, the high frequency components in the fault line are opposite the sum in the health lines. This characteristic can be used also for line selection. In fact, the high frequency components are not only produced by the transient, but also produced by the nonlinearity of the fault resistor R_G. If R_G is varying and nonlinear, such as in arcing fault, the high frequency components will be abundant. This circumstance is very common in the SCGF faults.

Furthermore, at the beginning of the fault, the current in the coil is almost zero, the abrupt changing component of the current in the fault line is almost opposite the sum of that in the health lines. Therefore, the abrupt changing components are another useful characteristic for line selection.

III. CALCULATION OF THE FAULT MEASURES

A. THE FAULT MEASURES

In short circuit faults, the obvious characteristics are the great short currents. This characteristic is enough for protection. Conventional protection device is unit structured; an individual device monitors and is responsible for one line only. Due to the weakness of the fault quantities in SCGF, no unique characteristic is great enough for fault line selection, the integrated selection scheme is employed in this paper. The integrated scheme samples and processes signals from all the feeders of a bus and implement fault selection according to information of all lines. As the signals are from all lines and the selection is based on the whole signals. More precise result can be obtained with the integrated selection scheme. With the integration of fault signal from all lines, the fusion algorithm of multi-fold fault components is occupied in this paper to enhance the reliability and adaptability of fault selection.

In order to realize the fusion of multifold fault components, the concept of fault measure is introduced. A fault measure is a nonnegative real variable assigned for each line to quantitatively estimate the likelihood to be the fault line. The fault measures are obtained using one-fold of the fault components. Each fault component corresponds to one different fault measure algorithm for each line. For example, if we employ 3 kinds of fault components for line selection, each line will obtain 3 fault measures. The ultimate selection result is concluded through fusion of all the fault measures. The current selection methods just use the qualitative expression to describe directly the judgment result based on one designated fault component while regardless of whether that component is strong enough. The fault measures are presented for each line to quantitively measure the likelihood of being the fault line. The likelihood degree for each line is calculated quantitively instead of presented the judgment result simply.

In compensated distribution, due to the compensation effect of the Peterson coil, the fundamental components are no more useful for line selection. The other fault components are used in the paper. These are transient component, abrupt changing component and damped DC component. All the components are the sum of the three phases, namely residue quantities. The following subsection describes the algorithms of fault measures for these fault components.

B. FAULT MEASURE ALGORITHM FOR TRANSIENT COMPONENTS

As mentioned above, if fault resistance is time varying and nonlinear, the fault currents will contain abundant high frequency non-stationary transients. The Peterson coil behaves high impedance for the high frequency transients. The high frequency components will therefore pass through the fault line to the health lines. Wavelet transform is a powerful tool for the high frequency non-stationary signals.

This paper employs dual-tree complex wavelet transform to separate the high frequency components from fault signals. In this application, the sampling frequency is 3200Hz; the lengths of original signal sequence are 2 cycles before the fault and 6 cycles after the fault. The algorithm of fault measures for high frequency transient components with wavelet transform are processed as follow.

Uses dual-tree complex wavelet to implement wavelet transform to the residue current of all lines with orthonormal algorithm. The merits of dual-tree complex wavelet include that it uses independent real and imaginary filters, without mutual interference; the transform of real part is lagging one sample cycle to the imaginary part, and so depress the information loss, and mitigate the frequency aliasing. 4 scales of wavelet decomposition are implemented to the signals in order the detail frequency bands are separated while the fundamental component do not be included just. The detail coefficients of real and imaginary parts of the dual-tree complex wavelet transform in the 4 scales are $DR_{1k}(i)$, $DR_{2k}(i)$, $DR_{3k}(i)$, $DR_{4k}(i)$, and $DI_{1k}(i)$, $DI_{2k}(i)$, $DI_{3k}(i)$, $DI_{4k}(i)$, respectively, where k is the number of the lines. The approximation coefficients of real and imaginary parts of the dual-tree complex wavelet transform in the 4 scales are $AR_{1k}(i)$, $AR_{2k}(i)$, $AR_{3k}(i)$, $AR_{4k}(i)$ and $AI_{1k}(i)$,

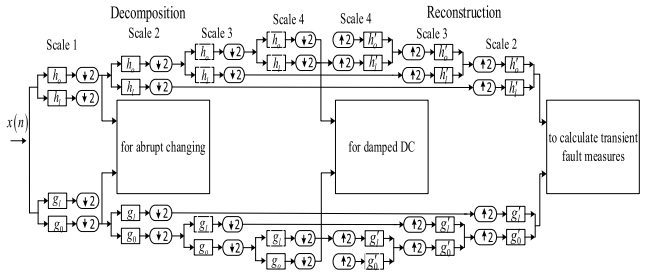

FIGURE 3. Flow chart of fault signal decomposition and reconstruct.

$AI_{2k}(i)$, $AI_{3k}(i)$, $AI_{4k}(i)$, respectively. After that, reconstructs the detail signals of scale 3 and scale 4 to scale 2. The purpose of this treatment is to make the coefficients with the equal gain in order to calculate the fault measure in the same scale. The reconstructed coefficients of real and imaginary parts are $RR_{22k}(i)$, $RR_{32k}(i)$, $RR_{42k}(i)$, and $RI_{22k}(i)$, $RI_{32k}(i)$, $RI_{42k}(i)$. The steps of using wavelet analysis are describe as in Fig. 3. In Fig. 3, the $x(n)$ is the original signal in residual form of each line; h_0, g_0 and h_l, g_l are the low-pass and high-pass functions of the real and imaginary wavelet transform decomposition; h'_0, g'_0, h'_l, g'_l is the reconstruction filter of low-pass and high-pass functions; symbols $\downarrow$ 2 and $\uparrow$ 2 represent down-sampling and up-sampling with dyadic respectively.

The original signal $x(n)$ is input into the wavelet decomposition algorithm with dual-tree complex wavelet. The detail coefficients of wavelet decomposition for scale 1 are mainly interference, while the approximation component is preliminary the signal. Through filtering of the wavelet, the approximation coefficients of real and imaginary parts in scale 1 are merged together as $AW_{1k}(i)$.

$$AW_{1k}(i) = \sqrt{(AR_{1k}(i))^2 + (AI_{1k}(i))^2} \tag{6}$$

This quantity is used to extract abrupt changing component as described in subsection C of this section. Similarly, the approximation coefficients of real and imaginary parts in scale 4 are merged for extracting damped DC as in subsection D of this section.

The fault measures of transient can be calculated according to the reconstructed wavelet coefficients to scale 2. Let the fault measures of transient for each line are $Fmt(k)$, the initial values are 0. Here k is still the number of lines and with $k = 0$ to symbol the bus. The real and imaginary parts of fault measures of transient are $Fmtr(k)$ and $Fmti(k)$, respectively. The coefficients of one cycle at the beginning and the end are abandoned to avoid the edge effect of the wavelet transform, and the remainder data is taken part in calculation. For each point, pick the real and imaginary parts of the reconstructed three coefficients with the maximal magnitude and satisfying a threshold. Take the real part as example, assuming the corresponding numbers are p, q and r. Then calculate the fault measures with the following rules:

1) If sign of coefficient in line p is opposite to the signs of line q and r, then the real part of fault measures for line p accumulate as in (7).

$$Fmtr(p) = Fmtr(p) + \left|RR_{s2p}(i)\right| \tag{7}$$

where, s is the number of scales, $s = 2, 3, \ and, 4$

2) If the signs of the three lines are the same, then the real part of fault measures for the bus accumulate as in (8).

$$Fmtr(0) = Fmtr(0) + \frac{1}{3}\left|RR_{s2p}(i) + RR_{s2q}(i) + RR_{s2r}(i)\right| \tag{8}$$

3) If only line p and q satisfy the threshold, and if the signs are opposite, it mean that one of p or q are fault line, but cannot be determined further, then half the incremental are accumulated as in (9) and (10).

$$Fmtr(p) = Fmtr(p) + 0.5 \cdot \left|RR_{s2p}(i)\right| \tag{9}$$

$$Fmtr(q) = Fmtr(p) + 0.5 \cdot \left|RR_{s2p}(i)\right| \tag{10}$$

If the signs of line p and line q are the same, it is equivalent to (8) while the magnitude of line r is zero. The real part of the fault measures for the bus is accumulated as in (11).

$$Fmtr(0) = Fmtr(0) + \frac{1}{3}\left|RR_{s2p}(i) + RR_{s2q}(i)\right| \tag{11}$$

4) If only line p satisfies the threshold, it is equivalent to (8) while the magnitude of line q and r is zero. Then the real part of the fault measures is accumulated as in (12).

$$Fmtr(p) = Fmtr(p) + \frac{1}{3}\left|RR_{s2p}(i)\right| \tag{12}$$

The real part of the transient fault measures is arrived for each line according to the accumulating algorithm point to point from scale 2 through scale 4 of the reconstructed coefficients.

Similarly, the imaginary part of the transient fault measures is arrived for each line as well. The total fault measures for transient are calculated by the composition of real and imaginary parts of the fault measures as in Equ. (13).

$$Fmt(k) = \sqrt{Fmtr(k)^2 + Fmti(k)^2} \tag{13}$$

C. FAULT MEASURES FOR ABRUPT CHANGING COMPONENT

The capacitance property of lines is susceptive to abrupt changing components while the reactance of Peterson coil is the converse. At the initiation of fault, the impedance of Peterson coil is almost infinite thus the current in the fault line is almost the opposite sum of current in the health lines. This case will generally maintain about half a cycle. At the beginning, the fault current is the opposite sum of the health currents. We call the waveforms at this period as abrupt changing components. The approximation of scale 1 as $AW_{1k}(i)$ is used to extract the abrupt changing component and calculate the fault measures of abrupt changing. The steps are as following:

1) Take the absolute value to the abrupt changing component of the current, and add them together for all lines. Search the sum of current for the peak value point as p. Let

the residual voltage in point p be V_p, the residual current in line k at point p be $I_p(k)$.

2) Obtain the sign of V_p variation, and calculate Equ. (14). As the current and the voltage are almost in differential relationship, at the peak value, the current in the fault line is opposite with the variation sign of the voltage, but the health lines are the same with the sign of the voltage. Therefore, the result in (14) will be negative for fault line and positive for health lines.

$$A(k) = I_p(k) \cdot sign(\Delta V_p) \tag{14}$$

3) The fault measure algorithm for the abrupt changing components is as in (15).

$$Fma(k) = \begin{cases} -A(k), & -A(k) > 0 \\ 0, & -A(k) \leq 0 \end{cases} \tag{15}$$

In Equ. (14), the A(k) corresponding to health lines is positive, the longer the lines are, the greater the quantities are. Thus, in Equ. (15), the fault measures are almost zero for health lines, and the longer lines correspond to more definite fault measures to zero. But for fault line, the fault measures are positive and the greatest.

D. FAULT MEASURES FOR THE DAMPED DC COMPONENT

As mentioned above, at the moment of the transient the damped DC component exists in Peterson coil and pass through the fault line. The magnitude of DC component is related to the angle of fault. It reaches the maximal if the angle of voltage is in zero, whereas, if the angle is 90 degrees, the DC component gets zero. Therefore, the damped DC component is random, and unreliable too.

The atom decomposition algorithm is employed in this paper to extract the damped DC component. The appropriations of wavelet transform in scale 4 are employed for DC component extraction. These signals are smooth enough to reduce the calculation amount of atom algorithm. For any signal y, it can be presented by linear combination of $g_{\gamma(m)}$ in D for M terms.

$$y \approx \hat{y} = \sum_{m=1}^{M} a_m g_{\gamma(m)}, \quad g_{\gamma(m)} \in D \tag{16}$$

where, $\gamma(m)$ is an indexing parameter associated with a particular dictionary element in D. Usually, the dictionary is over-complete. Namely, D has more elements than necessary to span the signal space. The match pursuit (MP) algorithm is usually used for atom decomposition. MP algorithm is a greed iterative algorithm for deriving signal in terms of chosen expansion functions from a dictionary. At each iteration, the algorithm found the most related atom from the dictionary according to the atom index. And then the atom is extracted from the original signal. This procedure is repeated until signal y has been extracted in enough precise.

In each iteration, MP searches for the atom $g_{\gamma(m)} \in D$, which has the largest inner product with the residual signal r_y^{m-1}. Then

$$r_y^m = r_y^{m-1} - \left\langle r_y^{m-1}, g_{\gamma(m)} \right\rangle g_{\gamma(m)} \tag{17}$$

The residual is r_y^m after $m-th$ iteration, then the original signal can be represented as the linear combination of m atoms.

$$y = \sum_{n=1}^{m} \left\langle r_y^{n-1}, g_{\gamma(n)} \right\rangle g_{\gamma(n)} + r_y^m \tag{18}$$

The atom dictionary can be constructed based on the features of the original signal to decrease the quantity of calculation. Such an atom dictionary is called coherent dictionary. In this application, we use damped DC atom dictionary.

$$f(t) = \sum_{q=0}^{Q-1} A_q \cos(2\pi f_q t + \phi_q) e^{-\rho_q (t - t_{sq})} \times [u(t - t_{sq}) - u(t - t_{eq})] \tag{19}$$

where A_q is the magnitude of the damped DC atoms; ρ_q is the damp coefficient; t_{sq} and t_{eq} are the start and end time of the function, respectively. The decomposition of damped DC atoms is first using MP algorithm to extract Gabor atoms, then using the obtained Gabor atoms to calculate the damped DC atoms.

In this application, the original signal is transformed by the dual-tree complex wavelet to divide into detail components and approximation components of real and imaginary parts with 4 scales. The composite components of real and imaginary parts of the approximation after 4 scales of wavelet decompositions, which contain the damped DC component still and are rather smooth by the filtering of wavelet, and therefore are advantage for atom algorithms. This signal is used in this paper to extract the damped components. Through the atomic decomposition to the approximation components with MP algorithm as discussed above, the polynomial terms with atom are derived. Then merge the atomic terms with the same attenuation coefficient together, and find the DC component with maximum energy for line selection. Let the chosen DC component in Peterson coil is D_L, the component with the same coefficient in line k is $D(k)$. The fault measures are constructed as Equ. (20).

$$Fmd(k) = \begin{cases} D(k) - |D_L - D(k)|, \\ \quad -D(k) - |D_L - D(k)| \geq 0 \\ 0, \quad -D(k) - |D_L - D(k)| < 0 \end{cases} \tag{20}$$

As we know, Prony method is similar to atoms. But Prony requires the signal continuous among the entire window, while the atom method does not. Single phase to ground faults are usually unstable, especially at the beginning of the fault. Unstable faults lead the fault signals discontinuous. Thus, the atom method is suitable for the discontinuity.

The fault measure algorithm for the three components has been established in the above sections. It is worth mentioning, the multi-fold fault components should be uncoupled each other. Otherwise, the coupled components will lead to

additional weight in the integrating procedure, and make the selection results excessively rely on them, thus bring detriment to the integrated result. Obviously, it is uncoupled between the transient and the DC components.

It is the similar between the abrupt changing component and the DC component. For relationship between the abrupt change and the transient, the former may contain some of the latter really, but the quantities are very little because of the calculation of abrupt changing component are very short moment. Therefore, it is approximately uncoupled between the abrupt change and the transient. Thus, all the used components in this paper are uncoupled.

IV. FUSION OF FAULT SIGNALS WITH EVIDENCE THEORY

A. EVIDENCE THEORY

Let $\Theta = \{H_1, H_2, \ldots, H_n\}$ be a group of hypotheses sets with thorough and mutually exclusive, which is called the frame of discernment. A function with $m(\cdot) : 2^{\Theta} \rightarrow [0, 1]$ is called BPA, and satisfies:

$$m(\Phi) = 0 \text{ and } \sum_{A \subseteq \Theta} m(A) = 1 \tag{21}$$

where Φ is the null set, A is any subset of Θ, and 2^{Θ} is the power set of Θ.

BPA is the basic belief assignment to hypotheses A. The assigned probability $m(A)$ indicates the belief assigned to A and represents the degree of the evidence supports the hypotheses A. The probability of full set Θ means the degree of assigned to unknow. The key algorithm of evidence theory is the combination of evidences from different sources as in (22).

$$m = m_1 \oplus m_2 \oplus \cdots \tag{22}$$

where $\oplus$ designates the combination. The rule of combination with m_1 and m_2 is defined as follows:

$$m(C) = \begin{cases} 0, & C = \Phi \\ K^{-1} \sum\limits_{A_i \cap B_j = C} m_1(A_i) m_2(B_j), & C \neq \Phi \end{cases} \tag{23}$$

$$K = 1 - \sum_{A_i \cap B_j = \Phi} m_1(A_i) m_2(B_j) \tag{24}$$

The preliminary way to tackle problems with ET is to establish frame of discernment firstly, and construct an algorithm for basic probability assignment. Then employ the combination rules to the BPA values and make the decision according to them.

B. FRAME OF DISCERNMENT FOR SCGF

The frame of discernment is the sets that composed of all basic decisions. In SCGF selection problems, the purpose is to select the fault line. Therefore, the frame of discernment is the sets of individual line as described in (25).

$$\Theta = \{\mathrm{L(k)} |\ \mathrm{k} = 0, 1, 2, \cdots, \mathrm{n}\} \tag{25}$$

where $L(k)$ is symbol line k. For k=0 corresponds to the bus.

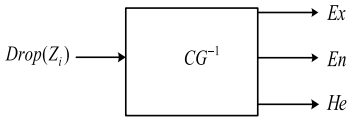

FIGURE 4. The reverse cloud generator.

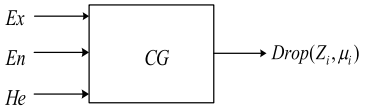

FIGURE 5. Forward cloud generator.

C. ESTABLISHMENT OF BPA FUNCTION

For line selection problem, the BPA function is determined by the fault measures of each line. The BPA function map the fault measures to intervals [0, 1] and the total sum equal to 1. Here we use data driven approach to produce the BPA. Cloud model is the transition tool for qualitative concept and quantitative data. In some cases, we have acquired a great amount of data for an event. The data are usually unprecise and rough. We need to arrive at a conceptual description on these data. This process is the transition from quantitative to qualitative. While in another cases, we have obtained the conceptual awareness on an event. But the conceptual notations are generally fuzzy and indefinite. We need to produce detail data complying with this notation. This process is the transition from qualitative concept to quantitative data. The cloud model algorithm can accomplish both these processes. The most typical cloud distribution is normal distribution. The algorithm to induce qualitative concept from historical samples is inverse cloud generators, as in Fig. 4. The algorithm of inverse cloud model is described as the following.

Let z_i represent the cloud droplets, namely the samples of data. The inverse cloud model uses 3 parameters to represent the notation, the expectation, the entropy, and the hyper entropy. The algorithms of calculating these parameters are as in Equ. (26), (27), (28), and (29), respectively.

$$Ex = \bar{Z} \tag{26}$$

$$En = \sqrt{\frac{\pi}{2}} \times \frac{1}{n} \sum_{i=1}^{n} \left| Z_i - \bar{Z} \right| \tag{27}$$

$$S = \sqrt{\frac{1}{n} \sum_{i=1}^{n} (Z_i - \bar{Z})^2} \tag{28}$$

$$He = \sqrt{S^2 - En^2} \tag{29}$$

The forward cloud generator is the opposite process towards the reverse cloud algorithm. The forward cloud generator accomplishes the generation of a number of droplets according to the concept. The forward cloud generator algorithm is shown in Fig. 5.

The conceptual diagram of a cloud model and the meaning of its parameters are shown in Fig. 6.

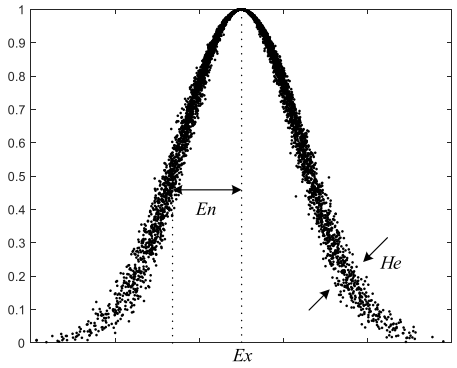

FIGURE 6. Digital characteristics of the cloud.

In the proposed SCGF integrated approach of line selection with ET, the BPA assignment is critical. We utilize the inverse cloud to process the historical data and acquire the cloud parameters with data driven approach. The historical data come from the practical fault data or simulations. The fault measures of each line are calculated firstly. Supposing the historical data are N. The fault measures for transient, abrupt changing and damped DC component are $Fmt(k)$, $Fma(k)$ and $Fmd(k)$, respectively. The parameters of cloud model as the expectation, the entropy and the hyper entropy are obtained from the known data of N dimension accordingly. For a SCGF, substitute the fault measures of the undetermined sample into the arrived cloud models. Suppose the memberships are $M_1(k)$, $M_2(k)$ and $M_3(k)$ corresponding to different fault measures in cloud model, the BPA functions are m_1, m_2 and m_3, m_1 correspond to the transients, m_2 to the abrupt changing, and m_3 to the DC component. Due to the memberships do not equal to 1 in sum, the BPA assignment functions have to be modified in the basis of the memberships as following.

$$m_1(k) = \frac{M_1(k)}{\sum_{k=1}^{N} M_1(k)} \tag{30}$$

$$m_2(k) = \frac{M_2(k)}{\sum_{k=1}^{N} M_2(k)} \tag{31}$$

$$m_3(k) = \frac{M_3(k)}{\sum_{k=1}^{N} M_3(k)} \tag{32}$$

where, N is the total number of lines in the same bus.

The steps of obtaining BPAs with cloud model can be summarized as following:

Step 1: Collect the historical data of single phase to ground faults. Calculate the fault measures for these data and build a cloud model with Equ. (26) through (29). The cloud is similar to in Fig.6. The horizontal axis is the fault measure, and the vertical axis is the membership of that sample. The parameters in Equ. (26)-(29) represent the cloud model established from the historical samples.

TABLE 1. Fault measures for various fault components.

	L1	L2	L3	L4	L5	L0(Bus)
Transient	3.66	8.52	0.388	2.22	0.83	5.38
Abrupt Chang	0.42	3.97	0.89	0.17	0.61	0.74
Damped DC	0.46	5.94	0.10	0.38	0.12	0.22

Step 2: Calculate the membership of the unknown sample. According to the fault measure of the unknown sample, calculate the membership based on the established cloud model parameters. Let the membership values for line k are M(k).

Step 3: Calculate the BPA of each line for each type of fault measure using Equ. (30)-(32) in order to let the BPAs obey the basic probability rules.

D. COMBINATION OF EVIDENCE

Fault measure algorithms for transients, abrupt changing and damped DC component are constructed above. Each algorithm corresponds to a BPA function as m_1, m_2 and m_3. Suppose $h_0 = \{L(0)\}$, $h_1 = \{L(1)\}, \ldots, h_k = \{L(k)\}$, meaning $L(k)$ is the fault line, and $k = 0$ means the bus as well. 3 groups of BPA are arrived as:

$$m_1(h_0), m_1(h_1), m_1(h_2), \ldots, m_1(h_k), m_1(\Theta)$$
$$m_2(h_0), m_2(h_1), m_2(h_2), \ldots, m_2(h_k), m_2(\Theta)$$
$$m_3(h_0), m_3(h_1), m_3(h_2), \ldots, m_3(h_k), m_3(\Theta)$$

The BPA represent the evidences of each line tends to be the fault line from different aspects. Through combination algorithm in Equ. (33), the integrated BPA is arrived to the common focused on evidences. Due to the common supported evidences reflect diverse fault characteristics, the common dominant fault components will be enlarged, and thus, the integrated method is robustness to the varying of fault circumstance.

$$m(h_k) = m_1(h_k) \oplus m_2(h_k) \oplus m_3(h_k) \tag{33}$$

The evidences combination algorithm obeys (23) and (24).

V. CASE STUDY

A. PRELIMINARY SIMULATION TO VALIDATE THE ALGORITHM

Numerous simulation tests were carried out for SCGF fault in distribution to test the correctness of the proposed fault selection algorithms. The simulated network is with 10kV nominal voltage, 5 lines, neutral compensated with a Peterson coil of overcompensated about 10%. The fault occurs at line 2. The fault angle is 30 degrees corresponding to the fault phase voltage. The simulations are conducted with RT-Lab. Fig. 7 gives the waveforms. The fault measures of each line in this simulation are shown in Table 1. It can be seen that the fault measures in fault line L2 is the greatest, which verifies the correctness of the preliminary algorithm of the fault measures.

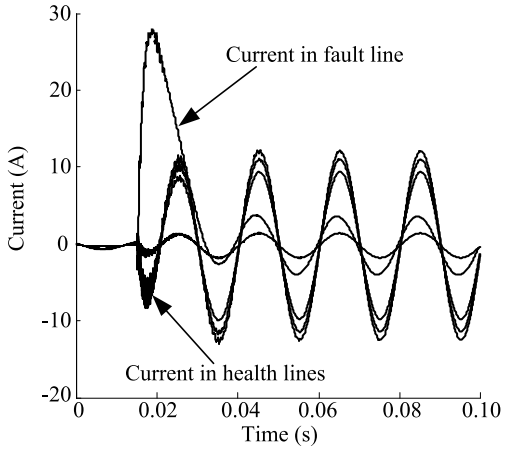

FIGURE 7. Waveform of SCGF simulation for compensated distribution.

TABLE 2. Line parameters of the model.

Line types	Resistance/(Ω/km)		Inductance/(mH/km)		Capacitance/(μF/km)	
	Positive sequence	Zero sequence	Positive sequence	Zero sequence	Positive sequence	Zero sequence
Cable	0.200	0.900	0.255	1.109	0.376	0.276
Overhead line	0.170	0.320	1.107	3.560	0.155	0.006

TABLE 3. Basic probability assignment to each line and their combination.

	m(L1)	m(L2)	m(L3)	m(L4)	m(L5)	m(L0)	m(Θ)
m1 (Transient)	0.06	0.49	0.00	0.12	0.00	0.14	0.19
m2 (Abrupt)	0.02	0.60	0.00	0.00	0.00	0.09	0.29
m3 (Damped DC)	0.04	0.69	0.00	0.09	0.00	0.01	0.17
m123	0.01	0.86	0.00	0.01	0.00	0.01	0.11

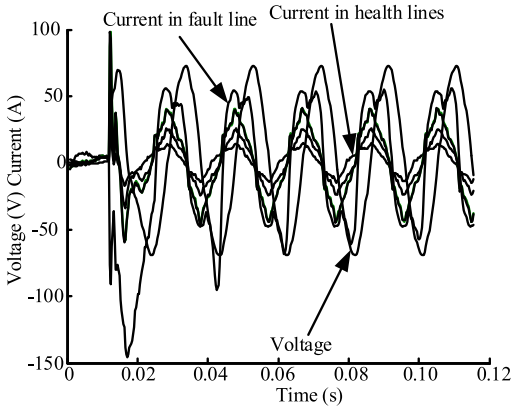

FIGURE 8. Example waveform of the fault.

B. LARGE AMOUNT OF SAMPLES FOR CONSTRUCTING THE CLOUD MODEL

Furthermore, to produce a great deal of samples in order to build the cloud model for subsequent analysis, the white noise as well as the power frequency interferences come from errors of the current transformers and unbalance of the network are imposed both to the signals. The quantities of noises and interferences are varied randomly for each simulation from 5% to 15% respectively. The simulations were randomly implemented for 1000 times in different circumstances. Each simulation results are regarded as labeled samples of a cloud droplet for training the cloud model. In each simulation, the parameters took different values in random. The length of each line varied from 3km to 6km randomly, cable and overhead line were combined randomly, the fault resistance varied from zero to 2 kilo-ohm randomly, and the arcing faults modeled in [29] were also conducted with different coefficients. The unit parameters of lines are listed in Table 2.

The simulation results are divided into fault lines and health lines. And the cloud models are trained employ these data according to Equ. (26), (27), (28) and (29). The accomplished cloud model for fault group as expectation, entropy and hyper entropy are [8.06, 2.53, 0.88], [3.96, 1.45, 0.24] and [4.83, 1.96, 0.57] for transient, abrupt change and damped DC, respectively. The cloud model for the health group as expectation, entropy and hyper entropy are [0.00, 0.53, 0.15], [0.00, 0.37, 0.04] and [0.00, 0.47, 0.13] for transient, abrupt changing and damped DC, respectively.

Using the accomplished cloud models, the fault measures in section A of this chapter were substitute to (30) through (32) to calculate the BPA. The BPA values for each line and each component are listed in Table 3. The combined BPA with D-S are also presented in Table 3. From the results we can see that the basic probability assignment of fault line was increased to $m(L2) = 0.86$, occupy predominant position in the whole lines. While the BPAs of health lines were decreased greatly. These results show that the combined algorithm of evidence theory possess the beneficial performance of focusing effect. This performance made the decision was based on multiple fault components instead of one component merely. The fault line is clarified further no matter which components are predominant. The robustness was improved thus.

C. REAL EXAMPLE TO VERIFY THE EFFECTIVENESS

The SCGF signals were acquired in a 10kV substation in Heilongjiang province of China. The substation is dual sectionalized single bus with 8 lines at each section of the bus. Fig. 8 gives waveforms of the fault. The sampling rate is 100kHz per channel in synchronous manner. The recorded fault data are inputted to the proposed algorithm. The corresponding fault measures and part of the BPA and their combination results are given in Table 4 and Table 5. For simplification, BPAs of only the predominant are listed

In Tab. 5, the combined results were that $m(L5) = 0.79$, the greatest, while the BPAs of the other lines are depressed. The decision of the algorithm indicates that line 5 is the fault line, which is consistent with the actual situation. This example proved the effectiveness of the proposed method in practice.

TABLE 4. Fault measures of each line for various fault components.

	Line1	Line2	Line3	Line4	Line5	Bus
Transient	0.18	0.21	0.22	0.19	12.4	8.4
Abrupt	2.95	1.86	1.33	1.93	5.27	2.38
Damped DC	1. 13	1.96	3.88	3.46	5.93	1.12

TABLE 5. The BPA for each line and their combination.

	m(L1)	m(L2)	m(L3)	m(L4)	m(L5)	m(L0)	m(Θ)
m_1 (Transient)	0.06	0.04	0.04	0.03	0.51	0.32	0.00
m_2 (Abrupt)	0.11	0.08	0.00	0.13	0.35	0.09	0.24
m_3 (Damped DC)	0.06	0.09	0.05	0.18	0.43	0.08	0.11
m_{123} (Combined)	0.02	0.01	0.01	0.03	0.79	0.05	0.12

TABLE 6. The results of the comparison.

Method	The transient	The integrated
Quantity of right	267	300
Rate of right	89%	100%

D. COMPARISON TO VERIFY THE ROBUSTNESS

The integrated method is compared with the individual-component-based methods. The simulations have been done at above-mentioned conditions for another 300 groups for comparison. Applying the simulation cases, the transient-based method [30] is compared with the proposed one. The transient method takes the same dual tree wavelet. Table 6 presents the results of the comparison. From the results we can conclude that due to the interferences, the selection of transient method was wrong in certain cases. But as the combination action of multifold components, the selection is more suitable for varying circumstance. Here we use robustness to evaluate the ability of the algorithm to adapt different fault circumstances. We can conclude from the results that, although single-signal based method was vague or even wrong in some cases, the integrated selections gives right and more clarified answer to indicate the fault line still. Therefore, the proposed integrated method exhibits remarkable advantage in robustness to the variation of fault circumstances than individual component-based method.

VI. CONCLUSION

Due to the weakness of fault signals, SCGF fault line selection in distributions is still an intractable problem. Due to the fault circumstances are complex and varied, individual component is not reliable for line selection. Especially for compensated distributions, as the fundamental components are no longer effective, selection of SCGF is even more difficult. This paper propose an ET based integrated selection method. Through the fusion of multi-fold fault components, the performances of selection are improved obviously. Using the fault measures, the likelihood of each line seems to be fault line are described in quantitative, thus achieve more flexible fusion. The transients are extracted by dual-tree wavelet, and the damped DC are extracted with atom algorithm. The construction of BPA functions is vital for fusion, this paper formulated them with cloud-model based data-driven approach, the results are objective. Case study shows that the investigated method is robust and practical.

Sometimes, one component may play a reactive role to fusion result if that component contains hardly any useful information. This paper provides only the fusion strategy for SCGF line selection, but which components in what conditions ought to participate in the fusion, are not answered still, such problems are worthy to research further.

REFERENCES

[1] Z. G. Datsios and P. N. Mikropoulos, "Safety performance evaluation of typical grounding configurations of MV/LV distribution substations," *Electr. Power Syst. Res.*, vol. 150, pp. 36–44, Sep. 2017, doi: 10.1016/j.epsr.2017.04.016.

[2] J. P. Nelson, "System grounding and ground-fault protection in the petrochemical industry: A need for a better understanding," *IEEE Trans. Ind. Appl.*, vol. 38, no. 6, pp. 1633–1640, Nov./Dec. 2002, doi: 10.1109/TIA.2002.804754.

[3] P. Y. Liu et al., "Fault line detection of flexible grounding system based on phase variation characteristics of zero-sequence current," *Power Syst. Tech.*, vol. 46, no. 5, pp. 1–9, May 2022, doi: 10.13335/j.1000-3673.pst.2021.2055.

[4] L. Rui, P. Nan, Y. Zhi, and F. Zare, "A novel single-phase-to-earth fault location method for distribution network based on zero-sequence components distribution characteristics," *Int. J. Electr. Power Energy Syst.*, vol. 102, pp. 11–22, Nov. 2018, doi: 10.1016/j.ijepes.2018.04.015.

[5] W. Wang, X. Gao, B. Fan, X. Zeng, and G. Yao, "Faulty phase detection method under single-line-to-ground fault considering distributed parameters asymmetry and line impedance in distribution networks," *IEEE Trans. Power Del.*, vol. 37, no. 3, pp. 1513–1522, Jun. 2022, doi: 10.1109/TPWRD.2021.3091646.

[6] M. Givelgerg, E. Lysenko, and R. Zelichonok, "Zero sequence directional earth-fault protection with improved characteristics for compensated distribution networks," *Electr. Power Syst. Res.*, vol. 52, no. 3, pp. 217–222, Dec. 1999, doi: 10.1016/S0378-7796(99)00032-2.

[7] O. Chaari, M. Meunier, and F. Brouaye, "Wavelets: A new tool for the resonant grounded power distribution systems relaying," *IEEE Trans. Power Del.*, vol. 11, no. 3, pp. 1301–1308, Jul. 1996, doi: 10.1109/61.517484.

[8] J. Meng, W. Wang, X. Tang, and X. Xu, "Zero-sequence voltage trajectory analysis for unbalanced distribution networks on single-line-to-ground fault condition," *Electr. Power Syst. Res.*, vol. 161, pp. 17–25, Aug. 2018, doi: 10.1016/j.epsr.2018.03.024.

[9] J. Li, Y. Li, W. Wang, J. Song, and Y. Zhang, "Fault line detection method for flexible grounding system based on changes of phase difference between zero sequence current and voltage," *Power Syst. Tech.*, vol. 45, no. 12, pp. 4847–4855, Dec. 2021, doi: 10.13335/j.1000-3673.pst.2020.2015.

[10] M. Wei, F. Shi, H. Zhang, H. Li, and W. Chen, "Feeder selection and section location of high impedance fault at resonant networks based on the phase differences between the synchronous harmonics of the zero sequence currents," *Proc. CSEE*, vol. 41, no. 24, pp. 8358–8372, Dec. 2021.

[11] G. Feng, T. Guan, L. Wang, Y. Xue, X. Yu, and B. Xu, "Grounding fault line selection of non-solidly grounding system based on linearity of current and voltage derivative," *Power Syst. Tech.*, vol. 45, no. 1, pp. 302–311, Jan. 2021, doi: 10.13335/j.1000-3673.pst.2019.1272.

[12] S. Di, Z. Hongwei, W. Lei, and J. Xiaozhen, "Research of fault line selection algorithm based on fuzzy theory for distribution network," in *Proc. 16th IET Int. Conf. AC DC Power Transmiss. (ACDC)*, 2021, pp. 275–282.

[13] S. Hao, X. Zhang, R. Ma, H. Wen, B. An, and J. Li, "Fault line selection method for small current grounding system based on improved GoogLeNet," *Power Syst. Technol.*, vol. 46., no. 1, pp. 361–368, Jan. 2022, doi: 10.13335/j.1000-3673.pst.2021.0256.
[14] Q. Shen, "A novel method of fault line selection in low current grounding system using multi-criteria information integrated," *Electr. Power Syst. Res.*, vol. 209, Aug. 2022, Art. no. 108010, doi: 10.1016/j.epsr.2022.108010.
[15] S. Vlahinic, D. Frankovic, B. Jurisa, and Z. Zbunjak, "Back up protection scheme for high impedance faults detection in transmission systems based on synchrophasor measurements," *IEEE Trans. Smart Grid*, vol. 12, no. 2, pp. 1736–1746, Mar. 2021, doi: 10.1109/TSG.2020.3031628.
[16] M. Wei, F. Shi, H. Zhang, Z. Jin, V. Terzija, J. Zhou, and H. Bao, "High impedance arc fault detection based on the harmonic randomness and waveform distortion in the distribution system," *IEEE Trans. Power Del.*, vol. 35, no. 2, pp. 837–850, Apr. 2020, doi: 10.1109/TPWRD.2019.2929329.
[17] Z. Wang, G. Song, Z. Chang, Z. Lei, C. Dang, Z. Wei, and H. Liu, "Real-time measurement of ground parameters and line selection method for single-phase grounding gault of distribution network," *Power Syst. Technol.*, vol. 38, no. 1, Sep. 2022, doi: 10.13335/j.1000-3673.pst.2022.1433.
[18] Z. H. Zhang and L. H. Wang, "Fault line selection method for small current grounding based on wavelet analysis and GA-SVM," *Autom. Instrum.*, vol. 36, no. 8, pp. 8–12 and 23, Jun. 2021, doi: 10.19557/j.cnki.1001-9944.2021.08.002.
[19] B. Hao, "Single-phase grounding fault line selection method based on zero-sequence current increment," *Energy Rep.*, vol. 8, pp. 305–312, Apr. 2022, doi: 10.1016/j.egyr.2021.11.196.
[20] B. Cai, Y. Liu, and M. Xie, "A dynamic-Bayesian-network-based fault diagnosis methodology considering transient and intermittent faults," *IEEE Trans. Autom. Sci. Eng.*, vol. 14, no. 1, pp. 276–285, Jan. 2017, doi: 10.1109/TASE.2016.2574875.
[21] X. Kong, B. Cai, Y. Liu, H. Zhu, Y. Liu, H. Shao, C. Yang, H. Li, and T. Mo, "Optimal sensor placement methodology of hydraulic control system for fault diagnosis," *Mech. Syst. Signal Process.*, vol. 174, Jul. 2022, Art. no. 109069, doi: 10.1016/j.ymssp.2022.109069.
[22] X. Kong, B. Cai, Y. Liu, H. Zhu, C. Yang, C. Gao, Y. Liu, Z. Liu, and R. Ji, "Fault diagnosis methodology of redundant closed-loop feedback control systems: Subsea blowout preventer system as a case study," *IEEE Trans. Syst., Man, Cybern., Syst.*, vol. 53, no. 3, pp. 1618–1629, Mar. 2023, doi: 10.1109/TSMC.2022.3204777.
[23] Q.-Q. Jia, C.-X. Dou, Z.-Q. Bo, N. Wang, and J. Tian, "An integrated phase to ground fault protection for neutral compensated power networks," in *Proc. IEEE Power Eng. Soc. Gen. Meeting*, vols. 1–10, Jun. 20077, pp. 1–8.
[24] J. Qingquan, Y. Qixun, Y. Wei, Y. Yihan, and S. Jiahua, "Multi-criteria relaying strategy for single phase to ground fault in MV power systems," in *Proc. Int. Conf. Power Syst. Technol.*, 2002, pp. 683–687.
[25] F. Deng, F. Xu, S. Feng, X. Zeng, Y. Huang, Z. Zeng, and Z. Zhang, "Research on high impedance fault detection method based on energy distribution characteristics of traveling wave full waveform," *Proc. CSEE*, vol. 42, no. 22, pp. 8177–8190, Nov. 2022.
[26] X. Zhu, X. C. Liu, and M. Y. Y. C. K. Liu, "Analysis and application of transient change of phase current under grounding fault in distribution network," *Automat. Electron. Power Syst.*, vol. 46, no. 24, pp. 187–196, Dec. 2022.
[27] L. Niu, G. Wu, and Z. Xu, "Single-phase fault line selection in distribution network based on signal injection method," *IEEE Access*, vol. 9, pp. 21567–21578, 2021, doi: 10.1109/ACCESS.2021.3055236.
[28] N. Wang, "Fault line selection of power distribution system via improved bee colony algorithm based deep neural network," *Energy Rep.*, vol. 8, pp. 43–53, Nov. 2022, doi: 10.1016/j.egyr.2022.10.070.
[29] W. Ren, Y. Xue, F. Yang, and B. Xu, "Modeling and analysis of arc grounding faults in isolated neutral distribution network," *Power Syst. Technol.*, vol. 45, no. 2, pp. 705–712, Feb. 2021, doi: 10.13335/j.1000-3673.pst.2019.2509.
[30] Q. Jia, P. Xiao, Y. Yang, L. Liu, and J. Song, "Wavelets method to select single phase faulted circuit for small current grounding power systems," *Relay*, vol. 29, no. 3, pp. 5–8, 2001.

JIE SUN was born in Heilongjiang, China, in December 1973. He received the M.S. degree from Northeast Electric Power University. He has been a Senior Engineer with State Grid Heilongjiang Electric Power Company Ltd., Qiqihar, China. His research interest includes fault line selection.

YAN WANG was born in Heilongjiang, China, in March 1970. He received the M.S. degree from Northeast Electric Power University. He has been a Senior Engineer with State Grid Heilongjiang Electric Power Company Ltd., Qiqihar, China. His research interests include fault line selection and the stability control of power systems.

YI SUN was born in Qiqihar, China, in May 1976. He received the M.S. degree from Northeast Electric Power University. He has been the Director of the Science and Technology Digitalization Department, State Grid Heilongjiang Electric Power Company Ltd., Qiqihar. His research interest includes fault line diagnosis.

FANGMING JIN was born in Heilongjiang, China, in September 1974. She received the M.S. degree from North China Electric Power University. She has been a Chief Marketing Engineer with State Grid Heilongjiang Electric Power Company Ltd., Qiqihar, China. Her research interest includes distribution network fault line selection devices.

XINYU GAO was born in Tangshan, China, in November 1999. He is currently pursuing the master's degree in electrical engineering with Yanshan University. His research interests include fault line selection and device.

QINGQUAN JIA was born in Jilin, China, in January 1970. He received the Ph.D. degree from North China Electric Power University. Since 2007, he has been a Professor with the School of Electrical Engineering, Yanshan University. His research interests include fault diagnosis for power systems and power quality.